J. Math. Biol. (1986) 24: 583-601

Journal of Mathematical Biology

Numerical solution of a nonlinear advance-delay-differential equation from nerve conduction theory

Henjin Chi*, Jonathan Bell** and Brian Hassard

Department of Mathematics, SUNY at Buffalo, Buffalo, NY 14214, USA

Abstract. A functional differential equation which is nonlinear and involves forward and backward deviating arguments is solved numerically. The equation models conduction in a myelinated nerve axon in which the myelin completely insulates the membrane, so that the potential change jumps from node to node. The equation is of first order with boundary values given at $t = \pm\infty$. The problem is approximated via a difference scheme which solves the problem on a finite interval by utilizing an asymptotic representation at the endpoints, cubic interpolation and iterative techniques to approximate the delays, and a continuation method to start the procedure. The procedure is tested on a class of problems which are solvable analytically to access the scheme's accuracy and stability, then applied to the problem that models propagation in a myelinated axon. The solution's dependence on various model parameters of physical interest is studied. This is the first numerical study of myelinated nerve conduction in which the advance and delay terms are treated explicitly.

Key words: Functional differential equation — Advance-delay-differential equation — Continuation method — Nerve conduction — Finite difference method — Numerical functional differential equation

1. Introduction

In this paper we solve a nonlinear, mixed-delay differential equation defined on the real line. The problem has the form

$$RC\frac{dv(t)}{dt} = \tilde{F}(v(t)) + v(t-\tau) + v(t+\tau)$$

$$-\infty < t < +\infty, \qquad v(-\infty) = 0, \qquad v(+\infty) = 1, \tag{1.1}$$

* *Current address*: Dept. of Math & CS, Pan American Univ., Edinburg, TX 78539, U.K.

** Supported in part by NSF Grant MCS8301724 and by a Biomedical Research Support Grant 2SO7RR0706618 from NIH

where $v(t)$ represents the transmembrane potential at a node in our simplified model for nerve conduction in a myelinated axon. The internodal delay τ, represents the reciprocal of the speed of the potential wave as it propagates down the axon. This constant τ is unknown a priori and must be found simultaneously with $v(t)$. The constants R and C represent axoplasmic nodal resistivity and nodal capacity, respectively. $\tilde{F}$ includes the model current-voltage relation.

In Sect. 2 we give a derivation of the model. In Sects. 3–6 we describe a numerical scheme with local truncation error of order four for solving (1.1). The problem is solved on a finite interval, with asymptotic approximations used outside the interval. The Eq. (1.1) is discretized by using a five point formula for the time derivative terms, and cubic interpolation for the delayed and advanced terms. We use finite difference methods to set up a system of $N+2$ equations to solve $N+2$ unknowns. Since the function $\tilde{F}$ is nonlinear, the Newton-Raphson iteration procedure was used to approach the solution. Because it is a nonlinear system, we need an initial guess of the solution. Using a test problem, which is solvable analytically, and a continuation method, we obtain the solution of the desired problem by using the exact solution of the test problem to start the continuation method. In Sect. 7 we present numerical results of the method. We test the accuracy of the method on several test problems. Then we apply the method to our specific model. We determine the dependence of the solution $v(t)$, and τ, on the various parameters b, a, R and C, and interpret the results.

2. Model formulation

Myelination of an axon allows it to conduct neuroelectric signals by exciting only a small percentage of membrane exposed to the extracellular medium at the node of Ranvier (see Fig. 1), particularly in the peripheral nervous system [3, 16]. This permits transmission at greatly reduced energy expenditure and higher speeds than comparably sized unmyelinated axons [16].

Because myelin has a higher resistance and lower capacitance than membrane, when the membrane is depolarized at a node, it tends not to depolarize the adjacent region of membrane, but instead it appears to jump to the next node to excite the membrane there [16] (called saltatory conduction). There have been a number of papers associated with mathematical modeling and examining various quantitative relations between model parameters [1, 2, 3, 12, 14, 15]. Most analytical studies have formulated a mathematical model from an electrical circuit model which assumes what we call the pure saltatory conduction (PSC) hypothesis, namely, the myelin has such high resistance, and low capacitance that it completely insulates the membrane.

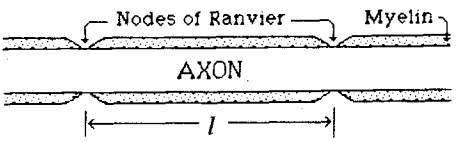

Fig. 1. Nodes of Ranvier

In a PSC model all excitable behavior is at the nodes and no transmembrane current is allowed through the internode. Consider the electrical circuit model given by Fig. 2. The r^i, r^o, V_k^i, V_k^o, j_k^i, j_k^o represent, respectively, the longitudinal resistances, longitudinal membrane potentials and currents across the kth node [13]. The superscript "i" (for inner) refers to axoplasmic quantities, the superscript "o" (for outer) refers to extracellar quantities, and the j_k^m represents membrane current at the kth node. Applying Kirchhoff's and Ohm's law to the circuit model, we then obtain:

$$r^i j_k^m = V_{k-1}^i - 2V_k^i + V_{k+1}^i \tag{2.1a}$$

$$-r^o j_k^m = V_{k-1}^o - 2V_k^o + V_{k+1}^o. \tag{2.1b}$$

Now let $R = r^i + r^o$, $V_k = V_k^i - V_k^o$. Then by subtracting (2.1b) from (2.1a), we obtain the following equation at the kth node:

$$Rj_k^m = V_{k-1} - 2V_k + V_{k+1}. \tag{2.2}$$

Now, as in [13], we suppose that the membrane current for the node is the sum of parallel capacity and ionic currents, thus giving

$$j_k^m = C\frac{dV_k}{dT} + I(V_k). \tag{2.3}$$

By combining Eqs. (2.2) and (2.3), we obtain the following difference-differential equation model of transmembrane potential V_k at the kth node:

$$\frac{V_{k-1} - 2V_k + V_{k+1}}{R} = C\frac{dV_k}{dT} + I(V_k). \tag{2.4}$$

In addition to the PSC hypothesis and the assumption concerning parallel capacity and ionic currents, the circuit model assumes that the axon is infinite in extent, that axon cross-sectional variations in potential (hence current) are negligible and that nodes are point sources of excitation, electrically identical and uniformly spaced.

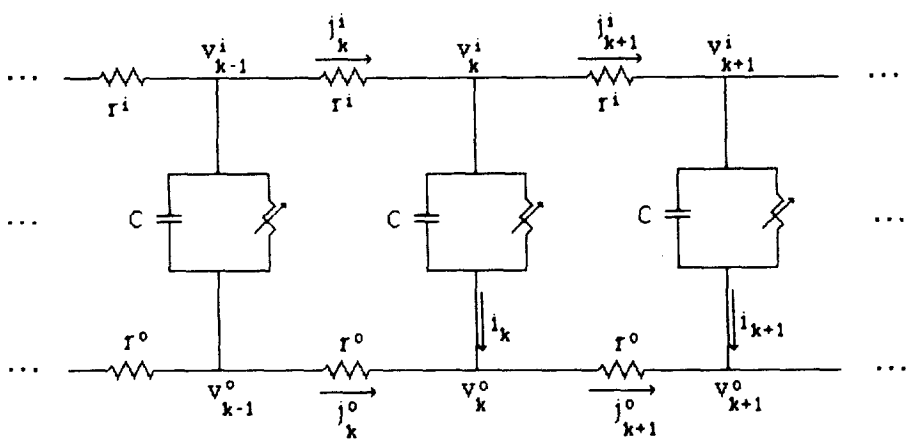

Fig. 2. Circuit for pure saltatory conduction model

At this point, various models can be studied depending upon what is chosen for the current-voltage expression $I(V)$. $I(V)$ may also depend upon other "state variables" satisfying their own voltage-dependent dynamics. For example, using a linear current-voltage relation, Landahl [12] showed there was a critical internodal length and diameter maximizing conduction velocity, while McNeal [14] computed strength-duration curves using a more physiologically realistic I. A more realistic model of the nodal membrane dynamics is one by Frankenhaeuser and Huxley [8], where their current-voltage relation $I(V)$ is the sum of three ion-specific current densities and a residual current. We choose the well known FitzHugh–Nagumo model [9] at each node since it has been used in studies of unmyelinated axons and has proven to be quite useful in exploring threshold behavior, action potential and repetitive activity. With FitzHugh–Nagumo dynamics for the nodal membrane, without a recovery term, system (2.4) becomes

$$\frac{V_{k-1}-2V_k+V_{k+1}}{R}=C\frac{dV_k}{dT}-F(V_k). \tag{2.5}$$

$F(V)$ is a current-voltage relation that has the nonlinear *cubic* behavior below:

$$F\in C^1[0,Q]; \qquad F(0)=F(Q)=0; \qquad F(x)<0 \quad \text{for } 0<x<P, \qquad F'(0)<0;$$
$$F(x)>0 \quad \text{for } P<x<Q, \qquad F'(Q)<0. \tag{2.6}$$

$V\equiv 0$ represents the rest potential, the threshold potential is represented by $V\equiv P$, and $V\equiv Q$ represents the fully-activated potential level of the node. Some analytical results for the model *with recovery* are given in Bell [2]. Below we concentrate on one representative function satisfying (2.6), namely $F(x)=Bx(Q-x)(x-P)$.

Now assume that a suprathreshold stimulus initiates a propagated action potential which then travels from node to node down the axon. Longitudinal circulating currents are set up which excite successive nodes. Because of the uniformity assumption, each succeeding node responds exactly as its predecessor except for an internodal time delay $\phi>0$; that is

$$V_{j+1}(T+\phi)=V_j(T) \quad \text{for all } j\in Z, \text{ all } T. \tag{2.7}$$

If l is the internodal length, the speed is given by $\vartheta=l/\phi$. One object here is to gain an understanding of how ϕ (and therefore ϑ) depends on other model parameters. Because of (2.7) we can consider the behavior at a single node, since the behavior at any other node is just a time translation. Letting $V(T)=V_k(T)$, then V satisfies

$$C\frac{dV(T)}{dT}=F(V(T))+\frac{V(T-\phi)-2V(T)+V(T+\phi)}{R} \tag{2.8}$$

with $V(-\infty)=0$, $V(+\infty)=Q$.

This problem is a nonlinear, mixed-delay, boundary value problem defined on the real line in which ϕ is unknown a priori. Before proceeding, we want to reduce parameters by nondimensionalizing (2.8). To nondimensionalize the model, let

$$t=\frac{T}{RC}, \qquad \tau=\frac{\phi}{RC}, \qquad v(t)=\frac{V(T)}{Q}. \tag{2.9}$$

With these substitutions, the model becomes

$$\frac{dv(t)}{dt} = f(v(t)) + v(t-\tau) - 2v(t) + v(t+\tau), \tag{2.10}$$

with $v(-\infty) = 0$, $v(+\infty) = 1$, where we obtain

$$f(v) = bv(v-a)(1-v),$$
$$a = P/Q, 0 < a < 1, \quad \text{and} \quad b = R \cdot B \cdot Q^2, b > 0. \tag{2.11}$$

Notice in (2.9), the scaling here is not the usual scaling in a cable model for nonmyelinated axon, but it serves our purpose.

In the nondimensional model, a is the threshold potential, τ is the nondimensional time delay, and b is related to the *strength of the ionic current density.* Since the current-voltage relation is just $f(v)$, once a node is "turned on", it cannot return to the rest potential $v = 0$. Therefore we expect the behavior of the solution at any node to be monotone increasing, that is, the solution to (2.10)-(2.11) represents a traveling front solution to (2.5)-(2.6).

3. Solution approximation outside the fixed interval

In this paper the class of problems of interest is

$$v'(t) = \frac{dv(t)}{dt} = f(v(t)) + v(t-\tau) - 2v(t) + v(t+\tau)$$
$$-\infty < t < +\infty, \quad \text{with } v(-\infty) = 0, \qquad v(+\infty) = 1. \tag{3.1}$$

Here f is $C^1[0, 1]$ and satisfies $f(0) = 0$, $f'(0) < 0$, $f(1) = 0$ and $f'(1) < 0$. We will later specialize to an f of the form given in Sect. 2. The constant delay must be found simultaneously with the solution. As mentioned in Sect. 2, we are looking for a monotone increasing solution $v(t)$ such that $0 < v(t) < 1$, for all t.

We first consider $t \leqslant -L$ with $v(t) \to 0, f(v(t)) \to 0$ as $t \to -\infty$. Using the Taylor expansion of f for x near 0, namely, $f(x) = a_1 x + a_2 x^2 + a_3 x^3 + O(x^4)$, the Eq. (3.1) becomes

$$v'(t) = \frac{dv(t)}{dt} = a_1 v(t) + a_2 v(t)^2 + a_3 v(t)^3 + v(t-\tau) - 2v(t) + v(t+\tau) + O(v^4). \tag{3.2}$$

Since $v(-L) \to 0$ as $L \to +\infty$, let $\varepsilon = v(-L)$ and consider the formal expansion

$$v(t) = \varepsilon u_1(t) + \varepsilon^2 u_2(t) + \varepsilon^3 u_3(t) + O(\varepsilon^4), \tag{3.3}$$

where we impose the condition

$$u_1(-L) = 1, \qquad u_2(-L) = 0, \qquad u_3(-L) = 0. \tag{3.4}$$

Substituting (3.3) into (3.2) and defining the operator L_τ by

$$L_\tau u(t) = u(t-\tau) + (a_1 - 2)u(t) + u(t+\tau),$$

we have the following equations

$$u_1'(t) - L_\tau u_1(t) = 0, \tag{3.5}$$
$$u_2'(t) - L_\tau u_2(t) = a_2 u_1(t)^2, \tag{3.6}$$
$$u_3'(t) - L_\tau u_3(t) = a_3 u_1(t)^3 + 2a_2 u_1(t) u_2(t). \tag{3.7}$$

Since the Eq. (3.5) is linear and homogeneous, we substitute $u_1(t) = e^{\lambda t}$ into the Eq. (3.5). This gives an equation for λ, namely,

$$\lambda + 2 - a_1 - 2\cosh(\lambda\tau) = 0. \tag{3.8}$$

Now since $a_1 = f'(0) < 0$, (3.8) has exactly two real roots, one positive and one negative. (Because we are interested only in monotone solutions in the present study, we consider only the real roots of (3.8).) Let λ_+ be the positive root of (3.8). Thus a solution to (3.5) which satisfies $u_1(-L) = 1$ and vanishes as $t \to -\infty$ is

$$u_1(t) = e^{\lambda_+(t+L)}. \tag{3.9}$$

A particular solution of the nonhomogeneous equation (3.6) is $u_2^p(t) = b_1 e^{2\lambda_+(t+L)}$, where

$$b_1 = \frac{a_2}{2\lambda_+ - a_1 + 2 - 2\cosh(2\lambda_+\tau)}.$$

A solution of (3.6), which satisfies $u_2(-L) = 0$, is then

$$u_2(t) = b_1(e^{2\lambda_+(t+L)} - e^{\lambda_+(t+L)}). \tag{3.10}$$

A particular solution of (3.7) is $u_3^p(t) = b_2 e^{2\lambda_+(t+L)} + b_3 e^{3\lambda_+(t+L)}$, where

$$b_2 = \frac{-2a_2b_1}{2\lambda_+ - a_1 + 2 - 2\cosh(2\lambda_+\tau)} = -2b_1^2, \tag{3.11}$$

and

$$b_3 = \frac{2a_2b_1 + a_3}{3\lambda_+ - a_1 + 2 - 2\cosh(3\lambda_+\tau)}. \tag{3.12}$$

A solution of (3.7) which satisfies $u_3(-L) = 0$ is then

$$u_3(t) = b_2 e^{2\lambda_+(t+L)} + b_3 e^{3\lambda_+(t+L)} - (b_2 + b_3) e^{\lambda_+(t+L)}. \tag{3.13}$$

Thus, for $t < -L$,

$$\begin{aligned} v(t) = {} & \varepsilon e^{\lambda_+(t+L)} + \varepsilon^2 b_1(e^{2\lambda_+(t+L)} - e^{\lambda_+(t+L)}) \\ & + \varepsilon^3(b_2 e^{2\lambda_+(t+L)} + b_3 e^{3\lambda_+(t+L)} - (b_2 + b_3) e^{\lambda_+(t+L)}) + O(\varepsilon^4). \end{aligned} \tag{3.14}$$

Next consider the right-hand expansion for $t > L$. With $v(t) \to 1$ and $f(v(t)) \to 0$ as $t \to +\infty$ consider the expansions

$$f(x) = A_1(1-x) + A_2(1-x)^2 + A_3(1-x)^3 + O((1-x)^4),$$

and

$$v(t) = 1 - \varepsilon_+ w_1(t) - \varepsilon_+^2 w_2(t) - \varepsilon_+^3 w_3(t) + O(\varepsilon_+^4),$$

with $v(L) = 1 - \varepsilon_+$, $0 < \varepsilon_+ \ll 1$. Using the same reasoning as above we obtain the sequence of problems

$$w_1'(t) - K_+ w_1(t) = 0, \qquad w_1(L) = 1, \tag{3.15}$$

$$w_2'(t) - K_+ w_2(t) = -A_2 w_1(t)^2, \qquad w_2(L) = 0, \tag{3.16}$$

$$w_3'(t) - K_+ w_3(t) = -A_3 w_1(t)^3 - 2A_2 w_1(t) w_2(t), \qquad w_3(L) = 0, \tag{3.17}$$

where K_τ is defined by $K_\tau u(t) = u(t-\tau) - (A_1+2)u(t) + u(t+\tau)$. Let $w_1(t) = e^{\lambda t}$, then substituting this into (3.15) yields the equation for λ, namely,

$$\lambda + 2 + A_1 - 2\cosh(\lambda\tau) = 0. \tag{3.18}$$

Since $A_1 = -f'(1) > 0$, (3.18) has exactly two real roots, one negative and one positive. Let λ_- be the negative root of (3.18). Thus the solutions to (3.15)-(3.17) are

$$w_1(t) = e^{\lambda_-(t-L)},$$
$$w_2(t) = B_1(e^{2\lambda_-(t-L)} - e^{\lambda_-(t-L)}),$$

where

$$B_1 = \frac{-A_2}{2\lambda_- + A_1 + 2 - 2\cosh(2\lambda_-\tau)},$$

and

$$w_3(t) = B_2\, e^{2\lambda_-(t-L)} + B_3\, e^{3\lambda_-(t-L)} - (B_2+B_3)\, e^{\lambda_-(t-L)},$$

where

$$B_2 = \frac{2A_2B_1}{2\lambda_- + A_1 + 2 - 2\cosh(2\lambda_-\tau)} = -2B_1^2,$$
$$B_3 = \frac{-2A_2B_1 - A_3}{3\lambda_- + A_1 + 2 - 2\cosh(3\lambda_-\tau)}.$$

Therefore, for $t > L$, with $\varepsilon_+ = 1 - v(L)$,

$$v(t) = 1 - \varepsilon_+\, e^{\lambda_-(t-L)} - \varepsilon_+^2 B_1(e^{2\lambda_-(t-L)} - e^{\lambda_-(t-L)})$$
$$-\varepsilon_+^3(B_2\, e^{2\lambda_-(t-L)} + B_3\, e^{3\lambda_-(t-L)} - (B_2+B_3)\, e^{\lambda_-(t-L)}) + O(\varepsilon_+^4). \tag{3.19}$$

4. The finite difference and interpolation schemes

Consider the following nonlinear mixed-delay problem

$$\frac{dv(t)}{dt} = f(v(t)) + v(t-\tau) - 2v(t) + v(t+\tau), \qquad -L \leqslant t \leqslant L, \tag{4.1}$$

with the following condition

$$v(0) = 0.5. \tag{4.2}$$

This equation is defined in a fixed interval, where f is nonlinear and $f(0) = f(1) = 0$. Since the equation is autonomous, time translates of solutions are also solutions. To fix the phase of the solution, we impose condition (4.2).

We use a fixed, uniform step size h in this scheme. We divided $[-L, L]$ into N equal size subintervals, letting $t_j = -L + jh$, $j = 0, 1, 2, \ldots, N$, where $N = 2L/h$ and approximate $v(t_j)$ by v_j. We adopt a fourth-order scheme to approximate the derivative term. From [4], we have

$$v'(t) = \frac{1}{12h}(v(t-2h) - 8v(t-h) + 8v(t+h) - v(t+2h)) + \frac{h^4}{30}f^{(5)}(\zeta),$$
$$\text{for some } \zeta,\ \zeta \in (t-2h,\ t+2h).$$

Thus, we have for the derivative term

$$v'(t_j) \approx \frac{1}{12h}(v_{j-2} - 8v_{j-1} + 8v_{j+1} - v_{j+2}). \tag{4.3}$$

For $j=0$ and $j=1$, terms v_{-2} and v_{-1} appear on the right-hand side of (4.3). In these cases, we use the approximate formula (3.14) for $t=-L-2h$ and $t=-L-h$ to approximate these terms. Similarly, for $j=N-1$ and $j=N$, terms v_{N+1} and v_{N+2} appear on the right-hand side of (4.3). We use (3.19) for $t=L+h$ and $t=L+2h$ to approximate these terms.

To approximate the delayed and the advanced terms in (4.1), we use cubic interpolation. Let $M=[\tau/h]$, where "$[x]$" means the integer part of x, and let $r=\tau-Mh$; note that $r \geqslant 0$. Then $t-\tau$ lies between $t-Mh-h$ and $t-Mh$. We use the cubic formula

$$v(t-\tau) = C_4 v(t-Mh-2h) + C_3 v(t-Mh-h) + C_2 v(t-Mh) + C_1 v(t-Mh+h) + \frac{9h^4}{324} f^{(4)}(\zeta), \quad \text{for some } \zeta,\ \zeta \in (t-Mh-2h,\ t-Mh+h),$$

where the C_i's are constants, given by

$$\begin{aligned} C_1 &= \frac{-(2h-r)(h-r)r}{6h^3}, \\ C_2 &= \frac{(2h-r)(h-r)(h+r)}{2h^3}, \\ C_3 &= \frac{(2h-r)(h+r)r}{2h^3}, \\ C_4 &= \frac{-(h+r)(h-r)r}{6h^3}. \end{aligned} \tag{4.4}$$

Thus, we have for the delayed term

$$v(t_j-\tau) \approx C_4 v_{j-M-2} + C_3 v_{j-M-1} + C_2 v_{j-M} + C_1 v_{j-M+1}. \tag{4.5}$$

When terms on the right-hand side of (4.5) have negative indices, formula (3.14) is used to approximate these terms. Similarly, we have for the advanced term

$$v(t_j+\tau) \approx C_4 v_{j+M+2} + C_3 v_{j+M+1} + C_2 v_{j+M} + C_1 v_{j+M-1}, \tag{4.6}$$

and when terms on the right-hand side of (4.6) have indices exceeding N, formula (3.19) is used to approximate these terms.

By using (4.3) to (4.6) to replace the derivative, delayed and advanced terms in the equation (4.1), the approximation scheme has a local truncation error of order four. The discretized version of (4.1) is then

$$\begin{aligned} &\frac{1}{12h}(v_{j-2} - 8v_{j-1} + 8v_{j+1} - v_{j+2}) - f(v_j) + 2v_j - C_1 v_{j+M-1} - C_2 v_{j+M} \\ &\quad - C_3 v_{j+M+1} - C_4 v_{j+M+2} - C_4 v_{j-M-2} - C_3 v_{j-M-1} \\ &\quad - C_2 v_{j-M} - C_1 v_{j-M+1} = 0, \quad \text{for } j = 0, 1, \ldots, N. \end{aligned} \tag{4.7}$$

In the system (4.7), the v_j's for $j<0$ are functions of v_0, and are evaluated by using (3.14) with $\varepsilon = v_0$, and neglecting the terms $O(\varepsilon^4)$. The v_j's for $j>N$ are functions of v_N, and are evaluated by using (3.19) with $\varepsilon_+ = 1 - v_N$ and neglecting the terms $O(\varepsilon_+^4)$.

In addition to the $N+1$ equations in (4.7), there is the condition

$$v_{N'} - 0.5 = 0, \quad \text{where } N' = [N/2] \tag{4.8}$$

which replaces (4.2), and in addition to the $N+1$ unknowns $v_0, v_1, \ldots, v_N$ there is the unknown delay τ.

5. Solution of the discretized system

There are many possible ways of solving the system (4.7), (4.8) for $v_0, v_1, \ldots, v_N$, and τ. If the Newton-Raphson scheme were used directly, the approximate τ would vary in each iteration step, and the coefficient matrix might vary in bandwidth because the integer M and the coefficients C_k, $k=1,\ldots,4$ depend upon τ. To avoid the potential for discontinuous change in M and the C_k's during the iteration, we designed a nested iteration scheme in which τ is fixed during the inner loop. The outer loop is the solution of an equation $g(\tau)=0$ by the secant method, where the function $g(\tau)$ is defined as follows:

Definition of $g(\tau)$. For fixed τ, we solve the system of $N+1$ equations

$$\begin{aligned} &(4.7) \quad \text{for } j = 0, 1, \ldots, N'-1 \\ &v_{N'} - 0.5 = 0 \\ &(4.7) \quad \text{for } j = N'+1, \ldots, N \end{aligned} \tag{5.1}$$

for $v_0, v_1, \ldots, v_N$. Then, we define $g(\tau) =$ *left-hand side of* (4.7) for $j = N'$.

This particular definition of $g(\tau)$ was arrived at after a certain amount of numerical experimentation. Unsuccessful attempts were made to solve the system (4.7) directly, and we tried to solve a modified version of (4.7) with the first equation replaced by a phase-fixing condition $v_0 =$ constant which was found to be ineffective. The system (5.1) applies the phase-fixing condition to the component $v_{N'}$ where it was found to be effective. Note that replacing the Eq. (5.1) for $j = N'$ with the equation $v_{N'} - 0.5 = 0$ preserves the band structure of the Jacobian matrix.

To approximate a solution to this nonlinear system (5.1), we use the Newton-Raphson scheme [5]. Given the initial approximation V^0, a sequence of iterates $\{V^k = (v_0^k, v_1^k, \ldots, v_N^k),\ k=0,1,\ldots\}$ is generated. This sequence converges to the solution provided that the V^0 is sufficiently close to the solution and the Jacobian matrix, J, is nonsingular at the solution.

The Jacobian matrix for the system (5.1) is a banded matrix with band width $2M+5$. In the numerical scheme, the Jacobian matrix was approximated by one-sided numerical differencing. The known band structure of the matrix was used to minimize the number of function evaluations required, and a banded matrix solver LEQT2B from the IMSL9 [10] was used to solve the linear systems at each stage in the Newton-Raphson iteration.

6. Continuation method

In the class of problems (3.1) we are considering, we have a test problem which we can solve exactly. This is (3.1) with the following expression for f:

$$f(v)=f_\vartheta(v)=\frac{1+2\vartheta(2v-1)-(1+\vartheta)(2v-1)^2-\vartheta(3-2v)(2v-1)^3}{2(1-\vartheta(2v-1)^2)}. \tag{6.1}$$

The solution to (3.1), (6.1) is $v(t)=(1+\tanh(t))/2$, $t\in R$, and $\tau=\tanh^{-1}(\sqrt{\vartheta})$. We may use this information and the continuation method (see [7, 19]) to solve other problems within our class of problems. Because we are solving a large system of nonlinear equations using Newton-Raphson method, it is very difficult to determine the initial guess which is close to the solution. So we take advantage of the test problem and continuation method to approach the solution we want. The way we use the continuation method on our class of problems is as follows. Consider the problem (3.1) with any nonlinearity $f_d(v)$ in our general class of f's which represents our "target problem", for which we desire the solution. We embed this problem in a one-parameter family of problems

$$\frac{dv(t)}{dt}=f_\alpha(v(t))+v(t-\tau)-2v(t)+v(t+\tau),$$

$$\text{with } v(-\infty)=0,\ v(\infty)=1, \tag{6.2}$$

$$f_\alpha(v)=\alpha f_\vartheta(v)+(1-\alpha)f_d(v), \qquad 0\leqslant\alpha\leqslant 1,$$

with $f_\vartheta(v)$ given by (6.1).

We compute solutions for α varying from $\alpha=1$ to $\alpha=0$. For $\alpha=1$, we are just solving the test problem for which the exact $v(t)$ and τ are known. This exact solution is used as the initial guess to solve the correspond discrete system (4.7). Once a problem for $\alpha>0$ is solved, we decrease α incrementally by $\Delta\alpha$ and use the solution to previous problem as the initial approximation to obtain the solution to the current problem. When we have solved the problem for $\alpha=0$, we are done.

We solved the problem (2.10) numerically by the scheme presented above on the CDC Cyber 815. We shall discuss the results in the next section.

7. Numerical results

In this section we present results of numerically solving (3.1) using a FORTRAN program which employs the method outlined in Sects. 3-6. To start with, we determine the accuracy of the method by applying our scheme to the test problem (6.1) with known solution. Then, we feed the continuation method with two different test problems from (6.1), whose solutions are also known so that we are sure of the accuracy of the continuation method. Having verified the convergence of our scheme with the continuation method, we solve our target problem (2.11), starting the continuation method from one test problem of the form (6.1). It is worth noting that we started the continuation method from three different test problems and for each case we approached to the target problem (2.11) and got the same solution. Then we consider the effects of parameter changes on the solution, and delay τ, of the Eq. (2.8) and (2.10).

Consider the following problem:

$$\frac{dv(t)}{dt} = f_\vartheta(v(t)) + v(t-\tau) - 2v(t) + v(t-\tau)$$

$$-\infty < t < +\infty \quad \text{with } v(-\infty) = 0,\ v(+\infty) = 1, \tag{7.1}$$

where f_ϑ is given by (6.1). This will be referred to as our test problem since, as we mentioned above, we know the solution and delay τ a priori. We use the scheme described above. We pick up a $\vartheta \in (1/3, 1)$ and replace the coefficients in Sect. 3 by their actual values. Choosing our test problem with $\vartheta = 0.35$, we have, analytically, the delay $\tau_{\text{exact}} = 0.680136$. For this problem we ran the program with $h = 0.1$, $N = 41$, $\varepsilon = 0.001$, $\vartheta = 0.35$, and $L = 2.0$. Since the system is nonlinear, we provide the initial guess of the solution to the iteration procedure by furnishing the program $N = 41$ mesh point values which came from the exact solution. Additionally, we need to find out τ by the secant method. Given $\tau_1 = \tau_{\text{exact}} + 0.001$ and $\tau_2 = \tau_{\text{exact}} - 0.001$, the program proceeds to iterate until the norm in the inner loop was less than 10^{-10} and the norm of τ in the outer loop is less than 10^{-8}. As the result, we obtained the solution, presented in Table 1, of the delay equation and $\tau = 0.6801398$ with the error between computed and exact delay being 3.5×10^{-6}. To check the accuracy and the stability of our scheme, we reduced h by one half, reran the program, and obtained $\tau = 0.6801364$, with the error being 1.6×10^{-7}. The solution of the second experiment and the exact solution are also included in Table 1 for comparison. Notice that we obtained the initial guess for $N = 81$ case by applying the cubic interpolation method to the solutions of $N = 41$ case. From Table 1, we conclude that the computed solution agrees with the exact solution to better than five digits. Moreover, since the difference between computed results of $N = 41$ and $N = 81$ is $O(10^{-6})$ which is within the error tolerance $O(10^{-4})$, we proceeded to use $N = 41$ in the rest of the calculations.

Table 1. Comparison of numerical solutions with the exact solution for $a = 0.05$, $b = 15.0$

T-Value	Exact solution	$h = 0.05$, $N = 81$	$h = 0.1$, $N = 41$
−2.00	0.01798621	0.01798693	0.01798640
−1.70	0.03229547	0.03229595	0.03229546
−1.40	0.05732418	0.05732449	0.05732348
−1.10	0.09975049	0.09975060	0.09974821
−0.80	0.16798162	0.16798139	0.16797676
−0.50	0.26894142	0.26894094	0.26893479
−0.20	0.40131234	0.40131199	0.40130841
0.00	0.50000000	0.50000000	0.50000000
0.20	0.59868766	0.59868791	0.59869026
0.30	0.64565631	0.64565659	0.64565901
0.40	0.68997448	0.68997476	0.68997652
0.70	0.80218388	0.80218401	0.80218224
1.00	0.88079708	0.88079715	0.88079408
1.40	0.94267582	0.94267590	0.94267389
1.80	0.97340301	0.97340309	0.97340216
2.00	0.98201379	0.98201387	0.98201329

Table 2. τ as a function of α as $\vartheta = 0.45$ in test problem for $N = 51$, $h = 0.2$

α	$\vartheta = 0.35$	$\vartheta = 0.4$
1.00	0.6801833932	0.7455460009
0.90	0.6943819718	0.7524306741
0.80	0.7082885743	0.7592620436
0.70	0.7219393996	0.7660430915
0.60	0.7353637053	0.7727765621
0.50	0.7485863969	0.7794649836
0.40	0.7616281482	0.7861107006
0.30	0.7745067270	0.7927158866
0.20	0.7872375064	0.7992825658
0.10	0.7998339241	0.8058071754
0.00	0.8122964720	0.8122964720

We now test the numerical scheme in conjunction with the continuation method by applying it to (7.1) and (6.1) with $\vartheta = 0.35$ for the initial test problem, and $\vartheta = 0.45$ for the problem to be solved. We set $\alpha = 1$ at the beginning, use the exact solution as initial guess for the problem, and choose a pair of numbers as the initial guesses of τ. The system is very sensitive and choosing too inaccurate a choice of inital guess of τ will cause the divergence of the solution. In the program run we set $N = 51$, $a = 0.05$, $b = 15.0$, $h = 0.2$, and $L = 5.0$. For each run, once we obtain the solution and τ of the delay equation, we decreased α by 0.1 and executed the iteration again. The same procedure was repeated until $\alpha = 0$. The solution and τ obtained are given in Table 2. Comparison of the computed solution and the exact solution is given inTable 3. We ran the same experiment over, starting with different test problems to see how sensitive the continuation method was to changes in the test problem. The initial test problem we adopted

Table 3. Comparison of numerical solutions with the exact solution

Time	Exact solution	Numerical solution	Error
−4.6	0.000101029	0.000101220	0.000000190
−3.6	0.000746029	0.000746685	0.000000656
−2.8	0.003684240	0.00368012	0.000001772
−2.0	0.017986210	0.017987145	0.000000935
−1.2	0.083172696	0.083142166	0.000030531
−0.6	0.231475217	0.231380294	0.000094923
−0.2	0.401312340	0.401253872	0.000058468
0.0	0.500000000	0.500000000	0.000000000
0.2	0.598687660	0.598727296	0.000039636
0.6	0.768524783	0.768512936	0.000011847
1.2	0.916827304	0.916793546	0.000033757
1.8	0.973403006	0.973391242	0.000011764
2.4	0.991837429	0.991835224	0.000002205
3.0	0.997527377	0.997527122	0.000000254
3.6	0.999253971	0.999254069	0.000000098
4.0	0.999664650	0.999664742	0.000000092

was (7.1) with $\vartheta = 0.4$. As predicted, it converged to the same $\tau = 0.81229647$ and we got the solution to agree with that of case $\vartheta = 0.35$ to better than 12 digits. In addition, from Table 3 we realize that the largest error is 0.94×10^{-4}. Therefore, we determined that the continuation method is accurate and in our experiment no matter which initial test problem we start with, we obtained the correct solution.

We then applied our numerical approach to the problem (2.10) with $f(v)$ presented in Sect. 2. The test problem employed is (6.1) with $\vartheta = 0.35$. Running the program with $a = 0.05$, $b = 15$, $h = 0.05$, $N = 41$, and $L = 1$, we obtained $\tau = 0.4351126$ and the solution, presented in Table 4, to the problem (2.10). Then we reran our program with $\vartheta = 0.40$ and 0.425 respectively in (6.1). Comparing the results obtained from using different ϑ's, we realized that for all the test problems we chose, we got the same τ, and the approximate solutions computed by the method starting from different test problems agree with each other to better than 12 digits (by using a good matrix solver, LEQT2B in IMSL9, with accuracy of 12 digits). The $\alpha - \tau$ relation graph for different ϑ's is exhibited in Fig. 3. The solution to (2.10) for $\vartheta = 0.40$ and 0.425 is included in Table 4 as well. To present the continuation procedure more clearly, the solution changes for different α's are shown in Fig. 4. The curves in $[-2, 2]$ represent the graph for $\alpha = 1$, 0.8, 0.6, 0.4, 0.2, 0.1 where $\alpha = 1$ is the initial test problem and $\alpha = 0$ is the target problem. Notice that the curves shrink and become more and more stiff as α decreases. Owing to the autonomous nature of this system, the program fixes the function value at $t = 0$, namely, $v(0) = 0.5$. According to the test results, we are convinced that in all cases the method will reliably give rise to solutions converging to the desired solution of (2.10).

Parameter changes will affect the behavior of the delay τ and the solution to the delay equation (2.10). Now we introduce some experiments of changing parameters a, b, R, and C and see what happens to the delay τ and equation solution. We will explain the behavior changes from the physiological point of view as well.

Table 4. Compare three numerical solutions from different test probem

T-Value	$\vartheta = 0.35$	$\vartheta = 0.4$	$\vartheta = 0.425$
−1.00	0.0071150078	0.0071150078	0.0071150078
−0.80	0.0174487830	0.0174487830	0.0174487830
−0.60	0.0426457062	0.0426457062	0.0426457062
−0.40	0.1022625067	0.1022625067	0.1022625067
−0.20	0.2369861873	0.2369861873	0.2369861873
−0.10	0.3480925348	0.3480925348	0.3480925348
−0.05	0.4186108238	0.4186108238	0.4186108238
0.00	0.5000000000	0.5000000000	0.5000000000
0.05	0.5900573033	0.5900573033	0.5900573033
0.10	0.6822976813	0.6822976813	0.6822976813
0.20	0.8338294908	0.8338294908	0.8338294908
0.40	0.9464838302	0.9464838302	0.9464838302
0.60	0.9785158465	0.9785158465	0.9785158465
0.80	0.9938335839	0.9938335829	0.9938335829
1.00	0.9977116701	0.9977116701	0.9977116701

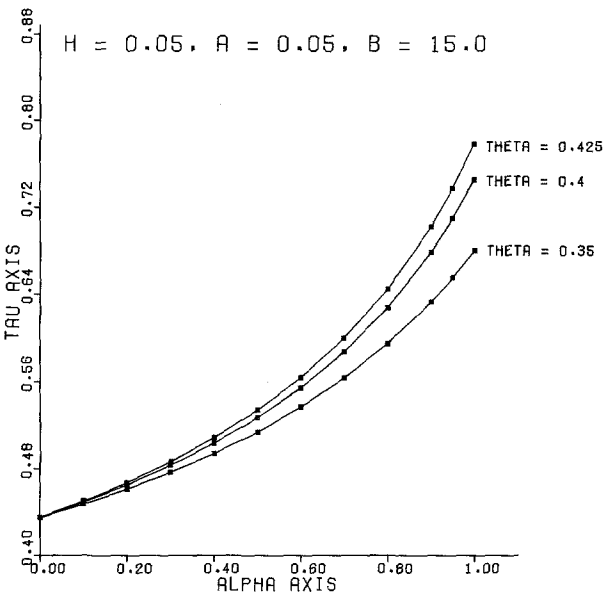

Figure 3. $\alpha - \iota$ relation when approach to target problem from $\theta = 0.35$, 0.4 and 0.425, respectively. With $h = 0.05$, $a = 0.05$, $b = 15.0$

We first examined how changes in the value of the threshold potential affected the rise time and the conduction speed of action potential. We fixed all other parameters by letting $h = 0.05$, $N = 41$, $b = 15$, and $L = 1$, and allowed the variable a to vary from 0.01 to 0.12 with increments of 0.01. As a decreases, the solution $v(t)$ becomes steeper in the middle and flatter on the ends. The change is shown in Fig. 5. This means the rise time of the membrane potential is faster for lower

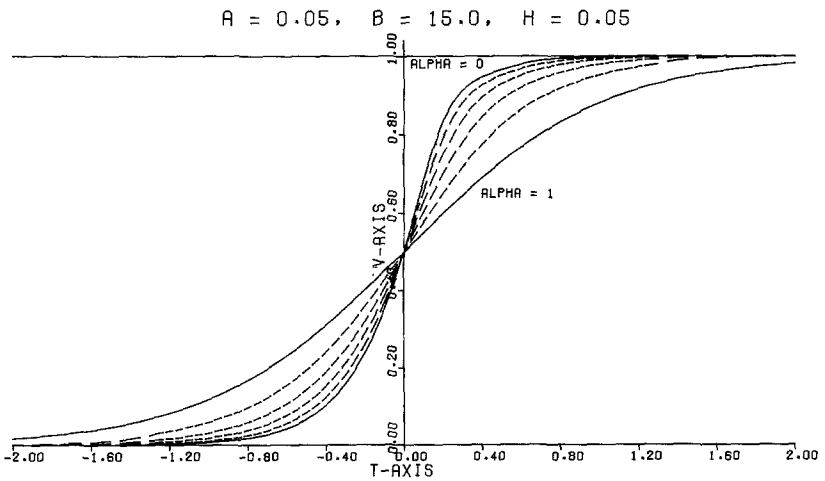

Fig. 4. Graph of solution changes when approaches to target problem from test problem with $\theta = 0.35$, $h = 0.05$, $a = 0.05$, $b = 15.0$

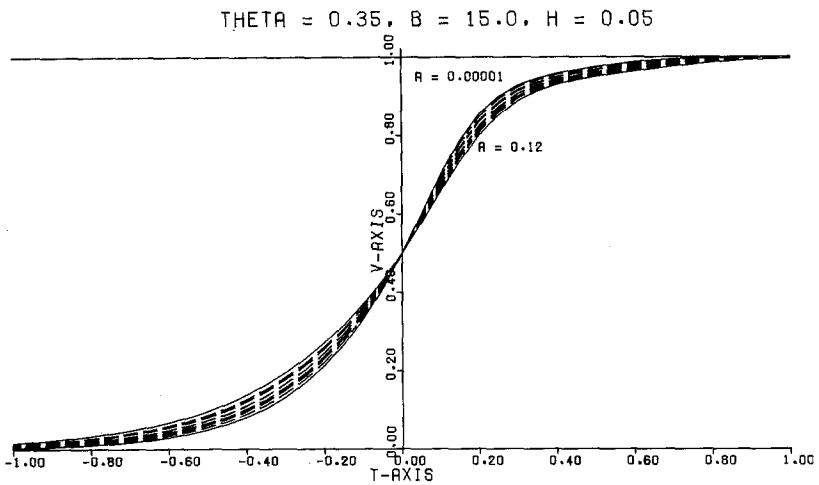

Fig. 5. Behavior of solution to target problem with different a's. With $h = 0.05$, $a = 0.05$, $b = 15.0$

threshold potential. We cannot directly compare this behavior to experimental observations becuse it is difficult experimentally to determine a precise value for threshold potential in real nodal membrane. Next consider the effect of threshold changes on the behavior of the conduction speed. From Table 5, we observe that the larger a is, the larger τ is. That is, all other parameters being fixed, an axon with higher threshold potential has lower conduction speed since the conduction speed is inversely proportional to internodal delay τ. Hence, axons with higher threshold potential have lower conduction speeds and slower rise times. This gives indirect consistent behavior to some experimental findings of Paintal [17] and Coppin and Jack (unpublished observations, see Jack et al. [11]), who found that action potentials (in myelinated fibers of cats) with slower conduction speeds have slower rise times. Since the model dynamics at the nodes is so simplified,

Table 5. τ as a function of a and b for $N = 41$, $h = 0.05$

a \ b	10.0	12.0	14.0	15.0	16.0	18.0	20.0
0.00	0.461650	0.423098	0.393128	0.380478	0.368953	0.348654	0.331413
0.01	0.472880	0.443713	0.403268	0.390294	0.378684	0.358161	0.340713
0.02	0.484613	0.444816	0.413843	0.400832	0.388994	0.368159	0.350447
0.03	0.496874	0.456427	0.424966	0.411679	0.388907	0.378684	0.360680
0.04	0.509680	0.468579	0.436601	0.423108	0.410936	0.389788	0.371478
0.05	0.523099	0.481315	0.448861	0.435131	0.422729	0.401420	0.382959
0.06	0.537145	0.494672	0.461716	0.447776	0.435177	0.413349	0.395064
0.07	0.551884	0.508699	0.475234	0.461091	0.448337	0.426082	0.407551
0.08	0.567361	0.523451	0.489472	0.475119	0.462159	0.439605	0.420675
0.09	0.583638	0.538982	0.504472	0.489920	0.476789	0.454130	0.434722
0.10	0.600759	0.555354	0.520318	0.505560	0.492261	0.469159	0.449702
0.11	0.618781	0.572639	0.537078	0.522212	0.508651	0.485323	0.465834
0.12	0.637808	0.590925	0.554830	0.539683	0.526230	0.502470	0.482761

we can make only qualitative comparisons with experiments, not quantitative ones.

Next we study the relationship between the strength of ionic current density, b, to the conduction speed and rise time of the membrane potential. We fix $h=0.05$, $N=41$, $a=0.05$, and $L=1.0$, and let b vary from 10 to 20 in unit increments. We notice that the smaller b is, the slower the solution rises (see Fig. 6). More specifically, if the strength of the ionic current density is lessened, the rise time of the membrane potential is slower, and τ is larger. Hence the conduction speed is larger when the strength of ionic current density is larger. Roughly interpreted, increasing the membrane conductance increases the conduction speed. We do not have experiments on myelinated axons to compare to this result directly, but it is known in studies on unmyelinated axons that increasing membrane conductances, for example imposing a higher density of sodium channels, lead to higher conduction speeds. Therefore all qualitative results seem to be consistent with experimental evidence as far as we can determine.

In the following, we study the behavior of the delay τ and the solution to (2.9) under the control of axoplasmic nodal resistance R and nodal capacitance C, where the model equation becomes

$$Cv'=f(v(t))+[v(t+\tau)-2v(t)+v(t-\tau)]/R.$$

To determine qualitatively the relationship between the nodal capacitance, C, to the conduction speed and rise time of the membrane potential, we fixed the nodal resistance R equal to 1 and let C vary from 0.7 to 1.3 in increments of 0.1. As seen in Fig. 7, the smaller C is, the faster the solution rises. This means that the rise time of the membrane potential is faster for lower nodal capacitance. From Table 6, we observe that when C increases τ increases. That is, if all other parameters are fixed, an axon with higher nodal capacitance has slower conduction speed. This is consistent with our intuition and known results on unmyelinated fibers that increasing the membrane capacitance tends to decrease conduction

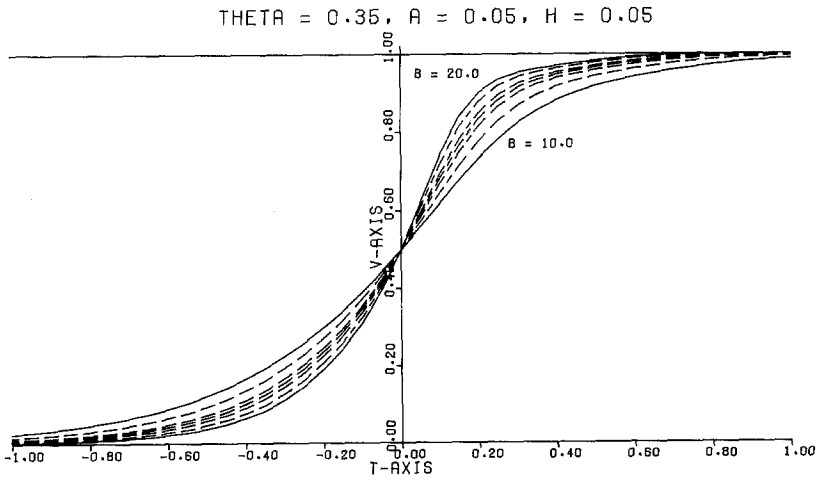

Fig. 6. Behavior of solution to target problem with different b's. With $\mathcal{O}=0.35$, $b=15.0$, $h=0.05$

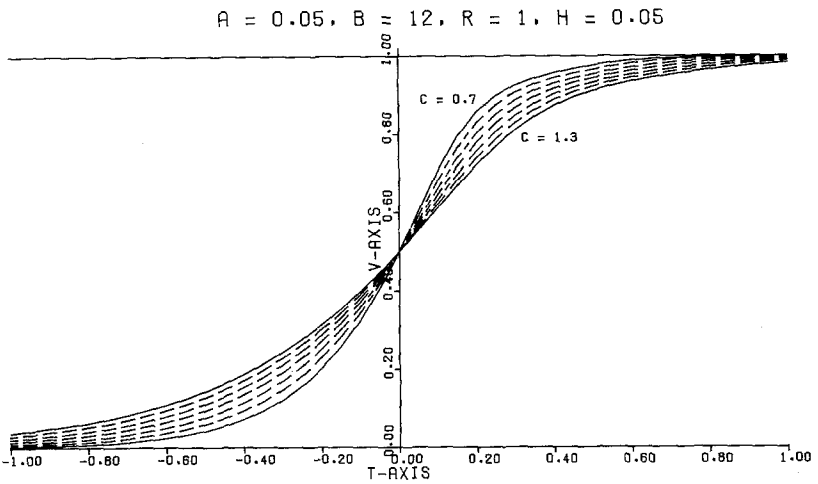

Fig. 7. Behavior of solution to target problem with different C's. With $a = 0.05$, $b = 12.0$, $R = 1$, $h = 0.05$

velocity. This result has also been verified by Moore et al. [15], who numerically examined the sensitivity of propagation speed on nodal capacity (see his Fig. 2). In their paper, they modelled the myelinated axon basically like an unmyelinated axon with spatially varying coefficients. Specifically, they allowed current leakage across the internodal regions, but this does not affect the qualitative dependence of conduction speed on nodal capacitance. It will, of course, have a significant quantitative effect. The above two observations of our model are also consistent with the previous observation that slower speed wave fronts have slow rise times.

Now consider the same model with the nodal capacity C fixed and resistivity R allowed to vary. For convenience we let $C = 1$ and varied R between 0.5 and 2.5. The numerical tests show us that when R decreases, the rise time of the solution decreases (see Fig. 8). In other words, the rise time of the membrane potential is faster for smaller nodal resistance. Again we observe from Table 6 that as R increases, so does τ. Hence we conclude that the higher nodal resistance will give rise to slower conduction speed and slower rise time in the action

Table 6. τ as a function of R and C for $a = 0.05$, $b = 12$, $N = 41$, $h = 0.05$

R \ C	0.7	0.8	0.9	1.0	1.1	1.2	1.3
0.50	0.232322	0.265792	0.299520	0.333515	0.367767	0.402093	0.436378
0.70	0.278036	0.318056	0.358196	0.398405	0.438538	0.478317	0.517602
0.90	0.318439	0.364144	0.409807	0.455201	0.500103	0.544044	0.586600
1.00	0.337213	0.385495	0.433638	0.481345	0.528202	0.573795	0.617932
1.10	0.355187	0.405923	0.456403	0.506202	0.554854	0.601895	0.647322
1.30	0.389011	0.444480	0.499231	0.552634	0.604308	0.653969	0.700613
1.50	0.420796	0.480439	0.538795	0.595164	0.649747	0.700887	0.751517
1.80	0.465205	0.530342	0.593325	0.653988	0.711529	0.767787	0.814118
2.00	0.492422	0.561355	0.627210	0.689966	0.749872	0.803210	0.855154
2.50	0.556866	0.632690	0.705463	0.772944	0.834156	0.892451	0.934432

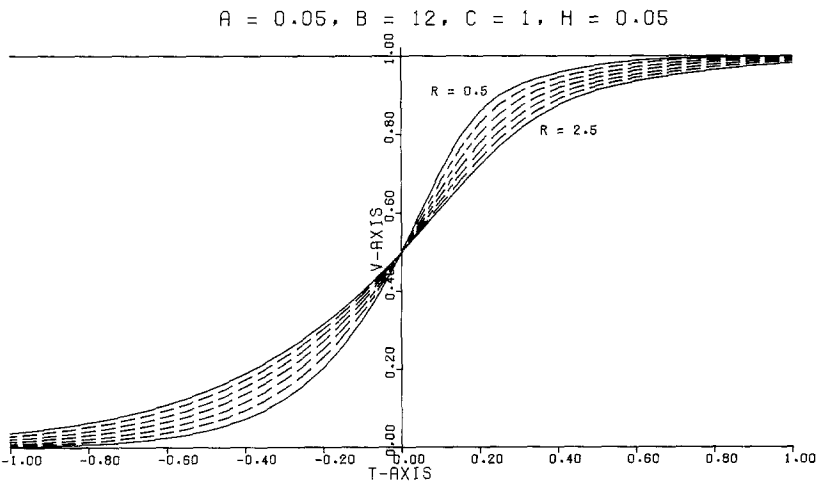

Fig. 8. Behavior of solution to target problem with different R's. With $a = 0.05$, $b = 12.0$, $C = 1$, $h = 0.05$

potential. Again this is consistent with the numerical results of Moore et al. [15], as well as previous work on unmyelinated axon modeling.

In summary, we have studied an extremely simple model of nerve conduction for myelinated axons and have found the parameter dependence results consistent with those of previous models and experiments. Of greater interest is our demonstration that the advance and delay terms which arise as a consequence of the traveling wave hypothesis in a saltatory model of myelinated nerve fiber can be treated explicitly, without considering other diffusion approximations.

Because the myelinated membranes do allow some transmembrane current to leak across, we have modified the above model to account for this current, and in particular, to consider the effect of myelin resistivity and capacitance. This work will be reported elsewhere.

References

1. Albus, J. S., Goldman, L.: Computation of impulse conduction in myelinated fibres: theoretical basis of the velocity-diameter relation. J. Biophys. **8**, 596-607 (1968)
2. Bell, J.: Some threshold results for models of myelinated nerves. Math. Biosci. **54**, 181-190 (1981)
3. Bell, J.: Behavior of some models of myelinated nerves. IMA J. Math. Appl. Med. Biol. **1**, 149-167 (1984)
4. Burden, R., Faires, J., Reynolds, A.: Numerical analysis, 2nd edn. Boston: Prindle, Weber, Schemdit Publishers, 1981
5. Carnahan, B., Luther, H., Wilks, J.: Applied numerical methods. New York: Wiley 1969
6. Cole, K. S.: Membranes, ions, and impulses. University of California Press, CA 1968
7. Deuflhard, P.: Stepsize control of continuation methods and its special application to multiple shooting techniques. Numer. Math. **33**, 115-146 (1979).
8. Frankenhaeuser, B., Huxley, A. F.: The action potential in the myelinated nerve fibre of Xenopus laevis as computed on the basis of voltage clamp data. J. Physiol. **171**, 302-315 (1964)
9. Hastings, S. P.: Some mathematical problems from neurobiology. Am. Math. Mon. **82**, 881-895 (1975)
10. IMSL User's Manual, IMSL Inc. (1982)
11. Jack, J. J., Noble, D., Tsien, R. W.: Electric current flow in excitable cells. Oxford: Oxford University Press 1975

12. Landahl, H. D., Podolsky, R. J.: Space velocity of conduction in never fibres with saltatory transmission. Bull. Math. Biophys. **11**, 19-27 (1949)
13. Mackey, M. C.: Ion transport through biological membranes. Berlin Heidelberg New York: Springer 1975
14. McNeal, D. R.: Analysis of a model for excitation of myelinated nerve. IEEE Biomed Eng. **23**, 329-337 (1976)
15. Moore, J. W., Joyner, R. W., Brill, M. H., Maxman, S. D., Najar-Joa, M.: Simulations of conduction in uniform myelinated fibres. Biophys. J. **21**, 147-159 (1978)
16. Morrel, P., Norton, W. T.: Myelin. Sci. Am. **242**, 88-118 (1980)
17. Paintal, A. S.: The influence of diameter of medullated never fibres of cats on the rising and falling phases of the spike and its recovery. J. Physiol. **184**, 791-811 (1966)
18. Strand, F. L.: Physiology: a regulatory system approach. New York: Macmillan 1978
19. Wasserstorm, E.: Numerical solution by the continuation method. SIAM Review, **15**, 89-119 (1973)

Received July 10, 1985/Revised July 27, 1986